ACS OMEGA

http://pubs.acs.org/journal/acsodf

Article

Facile Preparation of Robust Superhydrophobic/Superoleophilic TiO_2-Decorated Polyvinyl Alcohol Sponge for Efficient Oil/Water Separation

Zhiwei He,* Hanqing Wu, Zhen Shi, Zhe Kong, Shiyu Ma, Yuping Sun, and Xianguo Liu

Cite This: *ACS Omega* 2022, 7, 7084−7095

Read Online

ACCESS | Metrics & More | Article Recommendations | Supporting Information

ABSTRACT: Oily wastewater and oil spills pose a threat to the environment and human health, and porous sponge materials are highly desired for oil/water separation. Herein, we design a new superhydrophobic/superoleophilic TiO_2-decorated polyvinyl alcohol (PVA) sponge material for efficient oil/water separation. The TiO_2−PVA sponge is obtained by firmly anchoring TiO_2 nanoparticles onto the skeleton surface of pristine PVA sponge via the cross-linking reactions between TiO_2 nanoparticles and H_3BO_3 and KH550, followed by the chemical modification of 1*H*,1*H*,2*H*,2*H*-perfluorodecyltrichlorosilane. The as-prepared TiO_2−PVA sponge shows a high water contact angle of 157° (a sliding angle of 5.5°) and an oil contact angle of ∼0°, showing excellent superhydrophobicity and superoleophilicity. The TiO_2−PVA sponge exhibits excellent chemical stability, thermal stability, and mechanical durability in terms of immersing it in the corrosive solutions and solvents, boiling it in water, and the sandpaper abrasion test. Moreover, the as-prepared TiO_2−PVA sponge possesses excellent absorption capacity of oils or organic solvents ranging from 4.3 to 13.6 times its own weight. More importantly, the as-prepared TiO_2−PVA sponge can separate carbon tetrachloride from the oil−water mixture with a separation efficiency of 97.8% with the aid of gravity and maintains a separation efficiency of 96.5% even after 15 cyclic oil/water separation processes. Therefore, the rationally designed superhydrophobic/superoleophilic TiO_2−PVA sponge shows great potential in practical applications of dealing with oily wastewater and oil spills.

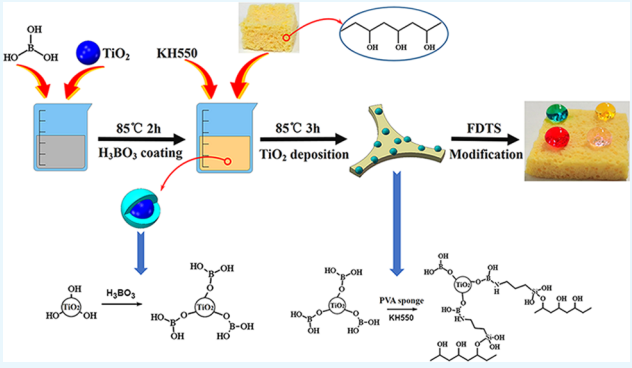

1. INTRODUCTION

Modern industries and frequent oil spill incidents have produced a large quantities of oily wastewater, which causes serious pollution in the environment.[1] The toxic chemicals in oily wastewater seriously threaten the survival of aquatic organisms, and some toxic substances enter the human body through the food chain and significantly influence human health.[2] To mitigate the threat of oily wastewater, traditional approaches have been utilized to purify oily wastewater, including controlled burning, air flotation, chemical dispersion, and bioremediation.[3,4] However, these methods suffer from secondary pollution, high cost, and low efficiency.[5,6] Thus, it is necessary to develop low-cost, environmentally friendly, stable, and efficient approaches or materials for the treatment of oily wastewater.

Bio-inspired from lotus leaves and insects, superhydrophobic materials (contact angle >150° and contact angle hysteresis <10°) have been widely investigated for many promising applications, such as anti-icing,[7−10] anti-corrosion,[11] sensor,[12] self-cleaning,[13,14] drag reduction,[15] and oil/water separation.[16] In recent years, various superhydrophobic materials have been developed and utilized for efficient oil/water separation, including meshes,[17] sponges,[18] textiles,[19] and filter papers.[20] Among them, superhydrophobic porous materials show the most stable and efficient properties for oil/water separation because of their large surface area, light weight, high stability, and high porosity.[21,22] Superhydrophobic porous materials usually possess three-dimensional (3D) structures and overcome the drawback of pore plugging present in the two-dimensional oil/water separation materials. To date, a series of 3D superhydrophobic porous materials with oil/water separation function have been achieved,[21] such as polyurethane sponges,[16] melamine sponges,[23] aerogels,[24,25] membranes,[26−28] fabrics,[29] and foam rubbers.[30]

Polyvinyl alcohol (PVA) sponge is a 3D porous material with low cost, high biocompatibility, and high porosity.[31] It is often used in the fields of tissue engineering,[32] adsorption

Received: November 30, 2021
Accepted: February 4, 2022
Published: February 14, 2022

https://doi.org/10.1021/acsomega.1c06775
ACS Omega 2022, 7, 7084−7095

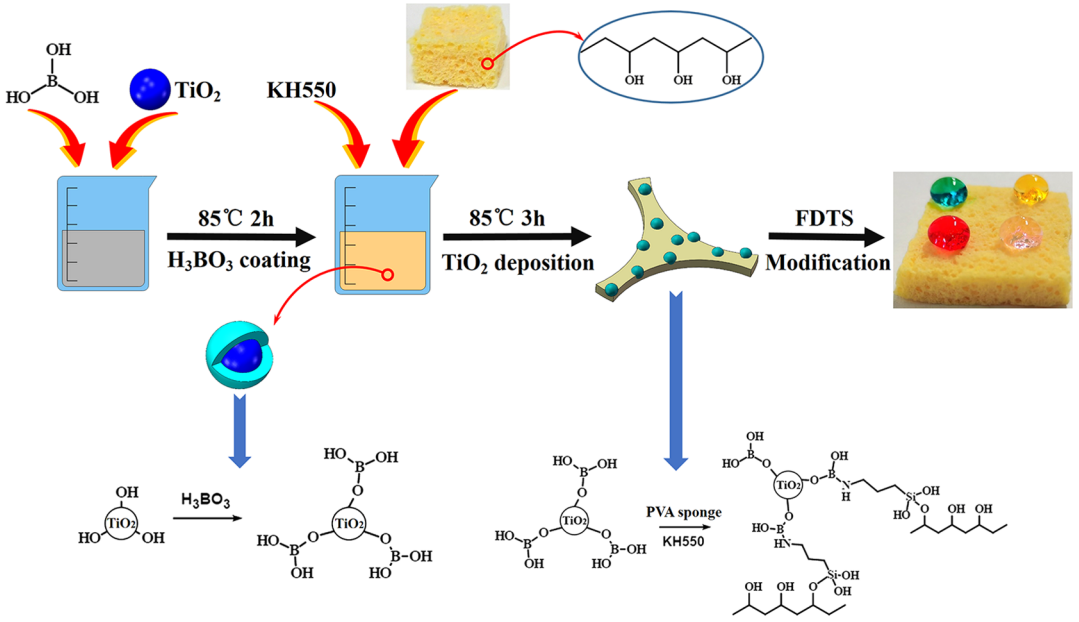

Figure 1. Schematic overview of preparing the TiO_2−PVA sponge.

materials,[33,34] and catalysts,[35] while there are only a few studies on superhydrophobic PVA-based sponges for oil/water separation.[36−39] For example, Chen et al. prepared a superhydrophobic PVA sponge by using a facile and environment-friendly route, and the as-prepared PVA sponge showed long stability for continuous oil/water separation.[36] Sha et al. reported that 3D superhydrophilic PVA-based composite sponges with high porosity can be used as efficient emulsion separation materials.[37,38] Wang et al. obtained a series of silane functionalized PVA formaldehyde sponges, which exhibited oil absorption capacities ranging from 4.0 to 14.0 $g{\cdot}g^{-1}$ in different solvents.[39] Wang et al. fabricated superhydrophobic PVA/Na_2SiO_3 porous materials and realized oil adsorption capacities ranging from 1.8 to 7.0 $g{\cdot}g^{-1}$ for different oil liquids.[40] Generally, pristine PVA sponge contains rich hydroxyl groups, which can help active sites to react with nanoparticles and thus obtain hierarchical structures on the skeletons of the PVA sponge. Besides, the durability of PVA-based sponges is also important for the long-term use of oil/water separation.[41] Shang et al. reported a superhydrophobic PDA-decorated melamine-formaldehyde sponge that still shows good superhydrophobicity after abrasion tests by a piece of sandpaper.[42] Wang et al. constructed superhydrophobic porous sponges by a mussel-inspired one-step strategy and evaluated the mechanical durability of the sponges by repeating the cycles of compression and release.[43] In short, superhydrophobic porous PVA sponges are promising porous materials and can be utilized for efficient oil/water separation.[44]

Herein, a new superhydrophobic/superoleophilic TiO_2-decorated PVA sponge material has been prepared for the first time for efficient oil/water separation, showing excellent chemical stability in harsh environments, thermal stability in boiling water, and mechanical durability after sandpaper abrasion test. Because of abundant hydroxyl groups of the PVA sponge, the as-prepared TiO_2−PVA sponge is successfully obtained by firmly anchoring TiO_2 nanoparticles onto the skeleton surface of pristine PVA sponge and chemically modifying with 1*H*,1*H*,2*H*,2*H*-perfluorodecyltrichlorosilane (FDTS), exhibiting a high water contact angle (WCA) of 157° (sliding angle of 5.5°) and an oil contact angle of ∼0°. More importantly, the as-prepared TiO_2−PVA sponge possesses excellent absorption capacity of oils (or organic solvents) ranging from 4.3 to 13.6 times its own weight. The TiO_2−PVA sponge also exhibits a separation efficiency of 97.8% for separating carbon tetrachloride from the oil−water mixture and maintains a separation efficiency of 96.5% even after 15 cyclic oil/water separation processes. Thus, the rational design of superhydrophobic/superoleophilic TiO_2−PVA sponge provides new insights into the practical applications of dealing with oily wastewater and oil spills.

2. RESULTS AND DISCUSSION

2.1. Preparation and Surface Morphology of the TiO_2−PVA Sponge. The schematic overview of the preparation of superhydrophobic/superoleophilic TiO_2−PVA sponge is illustrated in Figure 1. The whole process of preparing the TiO_2−PVA sponge mainly contains three steps. First, the H_3BO_3 and TiO_2 nanoparticles are added to the NaOH solution at pH = 10, and the reaction is carried out at 85 °C for 2 h. During this step, strong hydrogen bonds can be formed due to the rich hydroxyl groups of TiO_2 and three hydroxyl groups of H_3BO_3. Next, the silane coupling agent (KH550) and the TiO_2−PVA sponge are added to the resulting solution, and the reaction is continued under magnetic stirring.[45,46] The silane coupling agent usually acts as a bridge between the H_3BO_3 cross-linked TiO_2 nanoparticles and the pristine PVA sponge. The formation of N−B bonds between H_3BO_3 and KH550 can improve the cross-linking efficiency of TiO_2 nanoparticles onto the polymer chains.[47,48] In this process, the dehydration and condensation reaction between the hydroxyl groups Ti−OH and hydroxyl groups of the PVA sponge can enhance the formation of the TiO_2/PVA nanocomposite.[49,50] Besides, the cross-linking reaction of KH550 and H_3BO_3 can make TiO_2 nanoparticles firmly anchored on the skeletons of the pristine PVA sponge and thus construct rough micro-nanoscale structures. Finally,

https://doi.org/10.1021/acsomega.1c06775
ACS Omega 2022, 7, 7084−7095

the superhydrophobic/superoleophilic TiO_2−PVA sponge is obtained by lowering surface energy with an FDTS solution.

The morphologies of the pristine PVA sponge and the superhydrophobic/superoleophilic TiO_2−PVA sponge are shown in Figure 2. The inherent 3D porous structures of the

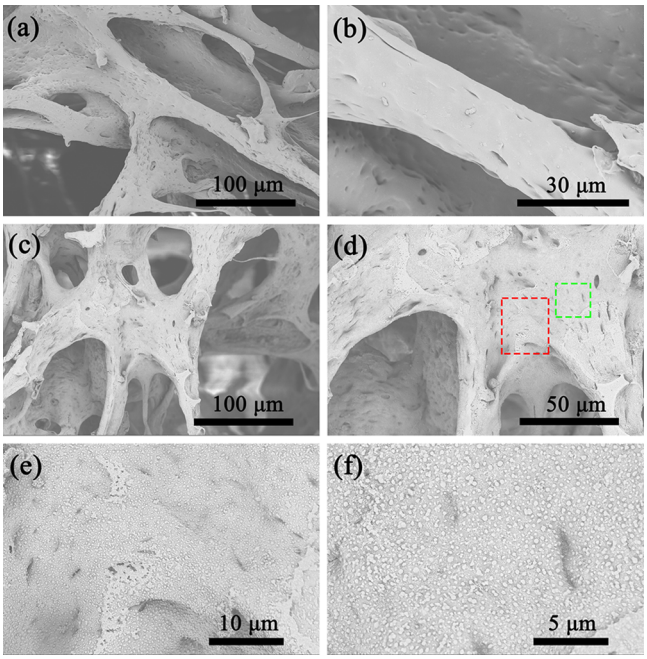

Figure 2. SEM images of the (a,b) pristine sponge and (c−f) superhydrophobic/superoleophilic TiO_2−PVA sponge with different magnifications. (e,f) correspond to the highlighted areas in red and green, respectively.

pristine PVA sponge with macro-scale pores are shown in Figure 2a. To evaluate the morphologies of the skeletons of pristine PVA sponge, a higher magnified image is displayed in Figure 2b, and it can be found that the skeleton of pristine PVA sponge is very smooth. After being modified with a low surface energy material (FDTS), rough porous structures of TiO_2−PVA sponge are formed, as illustrated in Figure 2c−f. The TiO_2−PVA sponge maintains the 3D porous structures of the pristine PVA sponge after the reaction and modification processes (Figure 2c), and the skeleton of the TiO_2−PVA sponge becomes rough. As shown in the highlighted areas in Figure 2d, TiO_2 nanoparticles are uniformly covered on the skeletons of the TiO_2−PVA sponge (Figure 2e,f), which is due to the deposition of TiO_2 nanoparticles cross-linked with H_3BO_3 and KH550.[46,47] Before the deposition process, the average size of TiO_2 nanoparticle dispersion in the presence of H_3BO_3 is about 48 nm, characterized using dynamic light scattering (Figure S2). Due to the cross-linking of KH550, TiO_2 dispersion becomes aggregated and finally forms TiO_2-based micro-structures (~0.22 μm) on the skeletons of the PVA sponge, as shown in Figure 2f. Thus, the obtained micro-nanoscale structures of the TiO_2−PVA sponge and the chemical modification of low surface energy give the TiO_2−PVA sponge superhydrophobicity and excellent water repellency.

2.2. Chemical Composition of the TiO_2−PVA Sponge. In order to confirm the chemical composition of the TiO_2−PVA sponge, energy-dispersive spectrometry (EDS) mapping, Fourier transform infrared (FTIR) spectra, and X-ray diffraction (XRD) pattern are analyzed in Figure 3. The EDS mapping of the TiO_2−PVA sponge is illustrated in Figure 3a. Compared with the elements of the pristine PVA sponge (i.e., C and O), the scan areas are almost covered by the elements of C, O, and B (Figure 3b−d), which means that H_3BO_3 has reacted and has been uniformly distributed on the skeletons of the pristine PVA sponge. Besides, it can be found that the EDS mapping (Figure 3b−f) and the EDS spectra (Figure 3g) of the TiO_2−PVA sponge contain the elements of F and Ti, indicating the successful deposition of TiO_2 nanoparticles and low surface modification of FDTS on the pristine PVA sponge.

The FTIR spectra of the pristine PVA sponge and the TiO_2−PVA sponge are shown in Figure 3h. As for the FTIR curve (black line) of the pristine PVA sponge, the typical peak at 3410 cm^{-1} is ascribed to the characteristic peak of rich hydroxyl groups of the PVA sponge. The observed peaks at 2860−2942 and 1002 cm^{-1} are due to the broad C−H alkyl stretching bands and the C−O stretching bands of the PVA sponge.[51] Another characteristic peak at 1658 cm^{-1} refers to the C═O band, which is possible due to the incomplete hydrolysis of poly(vinyl acetate).[52,53] The peaks at 1408 and 791 cm^{-1} are from the C−H bending and the stretching vibration of $-CH_2$.[54−56] Furthermore, the FTIR curve of the TiO_2−PVA sponge (red line) is also illustrated in Figure 3h. It can be found that the typical peak of hydroxyl groups of the TiO_2−PVA sponge significantly decreases because of superhydrophobicity. The peak at 476 cm^{-1} belongs to the stretching vibration of Ti−O,[49,57] indicating the deposition of TiO_2 nanoparticles on the skeleton of the PVA sponge. The absorption peaks at 1461 cm^{-1} are assigned to the B−O−B group,[46] and it means that H_3BO_3 has been successfully grafted onto the skeleton of the PVA sponge. The Ti−O−B band appears at 1398 cm^{-1}, showing that TiO_2 nanoparticles have successfully reacted with H_3BO_3.[58,59] Furthermore, the peaks at 1346 and 1131 cm^{-1} refer to the absorption band of N−B[47] and the stretching vibration of Si−O−C,[60,61] verifying that KH550 has reacted with the PVA sponge and TiO_2 nanoparticles have been firmly anchored onto the skeletons of the PVA sponge. In addition, the observed peak at 1242 cm^{-1} is due to the stretching vibration of the C−F group,[61,62] revealing the chemical modification of FDTS on the TiO_2−PVA sponge. Thus, the preparation of the TiO_2−PVA sponge has been demonstrated by the FTIR spectra when compared with that of the pristine PVA sponge.

The XRD patterns of the pristine PVA sponge and the TiO_2−PVA sponge are shown in Figure 3i. The XRD pattern of pristine PVA sponge displays a typical diffraction peak at 2θ = 19.5° and demonstrates the amorphous nature of the pristine PVA sponge.[63,64] After decorating with TiO_2, the XRD pattern of the TiO_2−PVA sponge shows peaks at 28.2, 36.8, 41.8, 44.8, 54.9, 57.4, 63.4, 65.0, and 69.9°, which is in agreement with the crystal form of rutile TiO_2 (PDF Card 88-1174).[65] In short, the XRD pattern of the TiO_2−PVA sponge shows the successful deposition of TiO_2 nanoparticles on the skeletons of the pristine PVA sponge.

2.3. Wettability of the TiO_2−PVA Sponge. The surface wetting properties of the pristine PVA sponge and the TiO_2−PVA sponge are shown in Figure 4. It can be seen that the water and oil droplets can be immediately absorbed into the pristine PVA sponge when they contact the pristine PVA sponge with superhydrophilicity and superoleophilicity (Figure 4a). For comparison, the modified TiO_2−PVA sponge exhibits

https://doi.org/10.1021/acsomega.1c06775
ACS Omega 2022, 7, 7084−7095

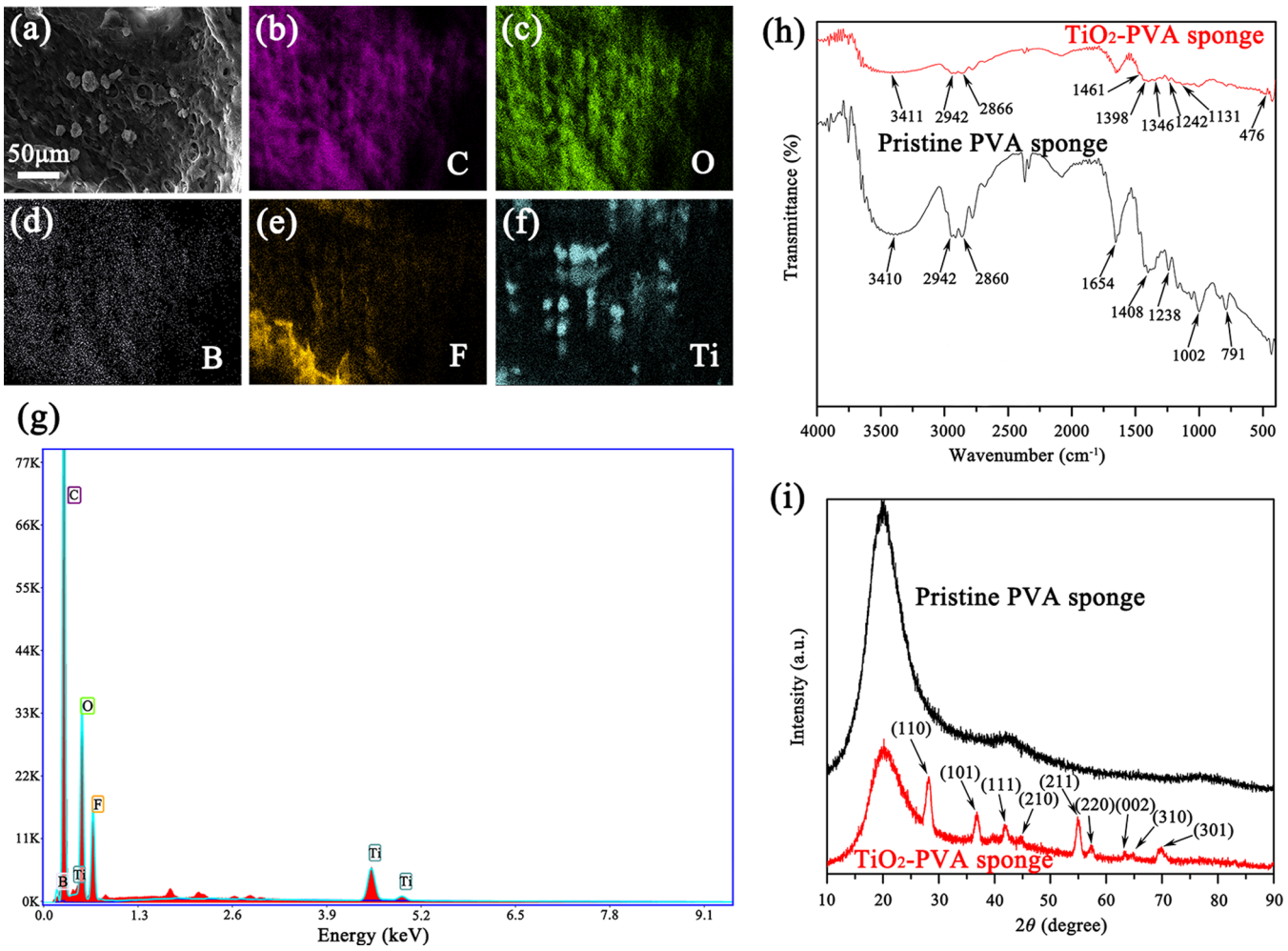

Figure 3. EDS mapping (a–f) and EDS spectra (g) of the TiO_2–PVA sponge; FTIR spectra (h) and XRD pattern (i) of the pristine PVA sponge and the TiO_2–PVA sponge.

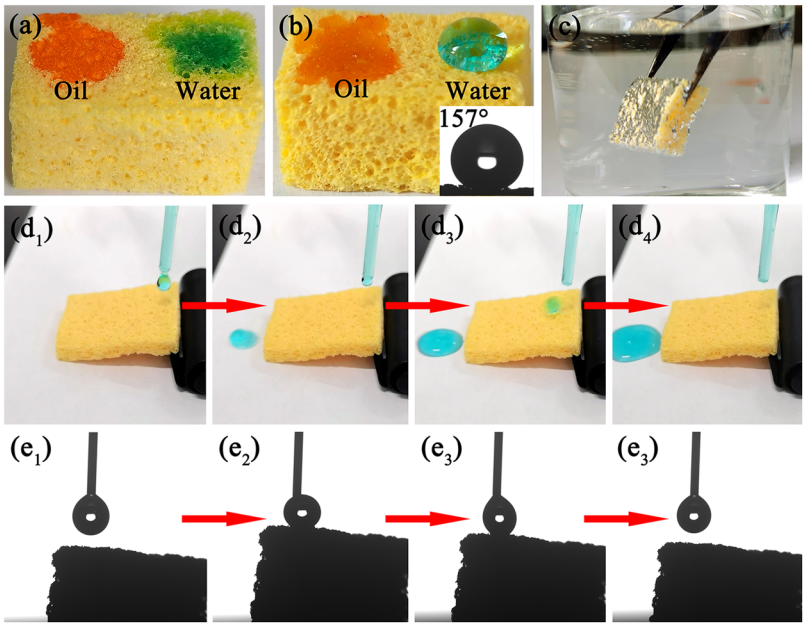

Figure 4. Images of the water droplet (dyed with Brilliant Green) and oil droplet (dyed with Sudan I) on the surface of the pristine PVA sponge (a) and the TiO_2–PVA sponge (b). (c) Mirror-like phenomenon of the TiO_2–PVA sponge when immersed in water. (d1–d4) Photographs of a water droplet sliding off from the TO_2–PVA sponge. (e1–e4) TiO_2–PVA sponge shows low adhesion for a water droplet.

https://doi.org/10.1021/acsomega.1c06775
ACS Omega 2022, 7, 7084–7095

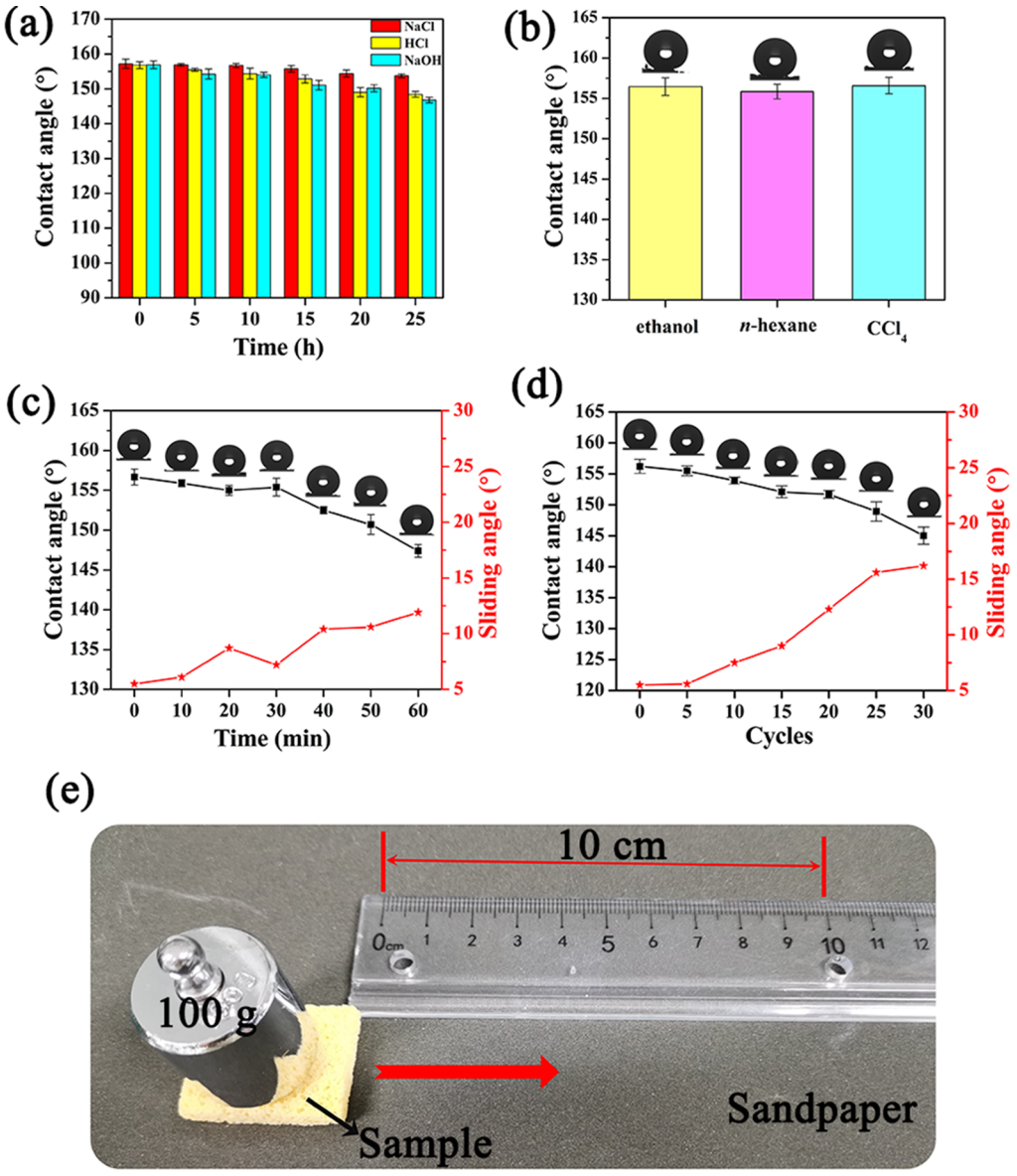

Figure 5. WCAs of the TiO_2−PVA sponge after being immersed in (a) 1 M NaCl solution, 1 M HCl solution, and 1 M NaCl solution for different times and (b) ethanol, *n*-hexane, and CCl_4 for 25 h. WCAs and sliding angles of the TiO_2−PVA sponge after (c) being immersed in boiling water for different times and (d) sandpaper abrasion test. (e) Schematic diagram of a sandpaper abrasion test.

different wettability. It can be seen from Figure 4b that the TiO_2−PVA sponge retains its superoleophilicity, while it shows superhydrophobicity for a water droplet (dyed with Brilliant Green). The water droplet shows a spherical shape on the TiO_2−PVA sponge, and its WCA is 157°. Interestingly, when the TiO_2−PVA sponge is completely immersed in water by an external force, a mirror-like reflection phenomenon can be observed due to the trapped air on the TiO_2−PVA sponge surface (Figure 4c). Moreover, the TiO_2−PVA sponge also exhibits ultra-low adhesion to water droplets. As shown in Figure 4d_1−d_4, the water droplet can easily slide off from the surface of the TiO_2−PVA sponge, showing a strong water repellent property. A water droplet can easily be detached from the surface of the TiO_2−PVA sponge when it comes in contact with the surface of the TiO_2−PVA sponge (Figure 4e_1−e_4). In the above discussion, the superoleophilicity and superhydrophobicity of the TiO_2−PVA sponge have been demonstrated.

2.4. Chemical Stability and Mechanical Durability of the TiO_2−PVA Sponge. Chemical stability is an important factor to characterize the TiO_2−PVA sponge for its real practical application. Herein, the chemical stability of the TiO_2−PVA sponge is tested by immersion tests in 1 M NaCl solution, 1 M HCl solution, and 1 M NaOH solution for different immersion times (0−25 h) (Figure 5a). The WCAs on the TiO_2−PVA sponge show a gradual continuous downward trend as the immersion time increases in different corrosive solutions. It can be seen from Figure 5a that the WCA (153°) on the TiO_2−PVA sponge shows a very small decrease after being immersed in 1 M NaCl solution for 25 h, indicating good chemical stability of the TiO_2−PVA sponge in 1 M NaCl solution. However, when immersed in 1 M HCl and 1 M NaOH solutions for 20 h, the WCA on the TiO_2−PVA sponge reduces to around 150° and continues to decrease with the increase in immersion time in the corrosive solutions. In the above harsh environments, the chemical stability of the

https://doi.org/10.1021/acsomega.1c06775
ACS Omega 2022, 7, 7084−7095

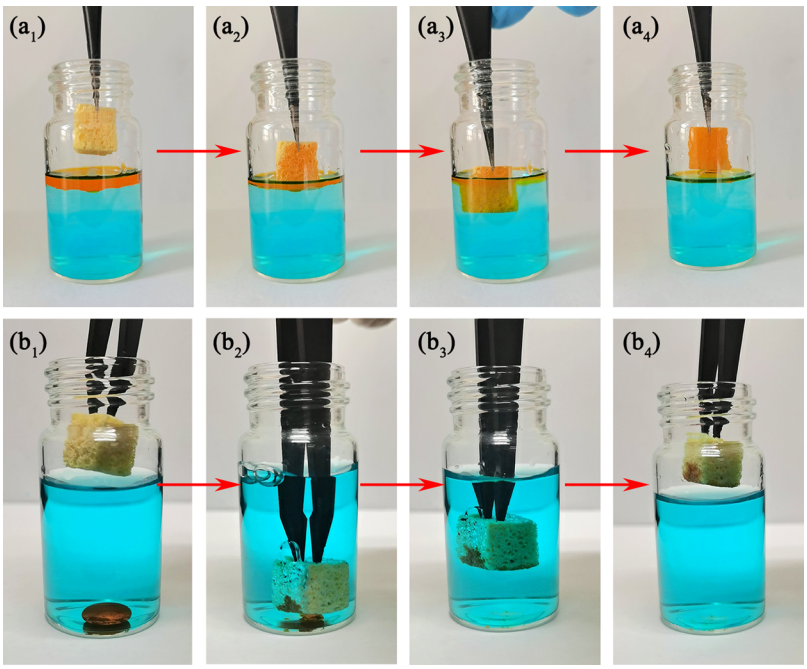

Figure 6. Images of the TiO_2−PVA sponge absorption process of (a1−a4) *n*-hexane (dyed with Sudan I) and (b1−b4) CCl_4 (dyed with Sudan I).

TiO_2−PVA sponge cannot remain for a long time (i.e., longer than 20 h), and thus, the corresponding mechanical durability of the TiO_2−PVA sponge can gradually decrease as time elapses. Generally, the TiO_2−PVA sponge possesses excellent chemical stability for solutions with different pH values. Besides, the solvent and oil resistance of the TiO_2−PVA sponge is evaluated by immersing the TiO_2−PVA sponge in ethanol, *n*-hexane, and tetrachloromethane (CCl_4) for 24 h (Figure 5b). It can be found that the WCAs are still above 155°, and the TiO_2−PVA sponge displays excellent solvent and oil resistance properties.

In addition, the thermal stability of the TiO_2−PVA sponge is investigated by immersing the as-prepared sponge in boiling water. The WCAs and sliding angles on the TiO_2−PVA sponge are illustrated in Figure 5c. It is found that the WCA and the sliding angle on the TiO_2−PVA sponge are 156.6 and 5.5°, respectively, at the beginning of the test. After being immersed in boiling water (0−60 min), the WCA drops to ∼150° at 50 min and deceases below 150° at 60 min, and the sliding angle gradually increases to about 11.9° at 60 min, indicating that the TiO_2−PVA sponge possesses good thermal stability in boiling water within 60 min.

The mechanical robustness of the TiO_2−PVA sponge is characterized by a sandpaper abrasion test, as shown in Figure 5d,e. The TiO_2−PVA sponge is placed under a load of 100 g on the sandpaper (800 mesh) (Figure 5e) and then is moved with a length of 10 cm for 30 cycles. It can be seen from Figure 5d that the sliding angle on the TiO_2−PVA sponge becomes more than 10° after 20 cycles, and the WCA on the TiO_2−PVA sponge reduces to 149° after 25 cycles. This means that the TiO_2−PVA sponge gradually loses its superhydrophobicity during the abrasion cycles. Similarly, Parsaie et al. found that the contact angle of the superhydrophobic polyurethane (PU) sponge does not show obvious changes after 10 cycles of abrasion tests.[2] You et al. reported that chitosan−PVA−TiO_2-coated copper mesh still maintains its superhydrophobicity after 25 cycles of abrasion tests.[17] Furthermore, ultrasonification is also used to evaluate the durability of the TiO_2−PVA sponge in ethanol for different times (i.e., 0−60 min). The results show that the contact angle on the TiO_2−PVA sponge remains above 150° (Figure S1), indicating its excellent superhydrophobicity and durability. In short, the as-prepared superhydrophobic/superoleophilic TiO_2−PVA sponge exhibits excellent chemical stability, thermal stability, and mechanical durability and thus shows great potential in the application of oil/water separation.

2.5. Oil Adsorption Performance of the TiO_2−PVA Sponge. The superhydrophobic/superoleophilic TiO_2−PVA sponge with high porosity can be used as an ideal material for efficient oil/water separation. Herein, the TiO_2−PVA sponge is used as an adsorption material to separate different oils mixed in water through selective absorption. To simulate a practical adsorption process, oils with different densities are utilized for absorption by the superhydrophobic/superoleophilic TiO_2−PVA sponge. It can be seen from Figure 6a_1−a_4 that the light oil (*n*-hexane dyed with Sudan I) floats on the surface of water (dyed with Brilliant Green). When the TiO_2−PVA sponge is forced to contact with *n*-hexane, it immediately absorbs *n*-hexane. Similarly, the TiO_2−PVA sponge can also be used to absorb heavy oil (CCl_4 dyed with Sudan I) from the bottom of the water, as shown in Figure 6b_1-b_4. In the whole absorption process, the TiO_2−PVA sponge is not contaminated by the Brilliant Green-dyed water, indicating that the superhydrophobicity of the TiO_2−PVA sponge can be maintained during the oil absorption process. Furthermore, obtaining absorbed oils from the TiO_2−PVA sponge is also important for the oil/water separation application. The absorbed oils with low viscosity in this study can be easily obtained by drying, while the recovery of oils with high viscosity can be realized by mechanically compressing, washing with anhydrous ethanol, and drying.[66,67]

2.6. Oil/Water Separation Performance of the TiO_2−PVA Sponge. Based on the above good oil absorption performances, the oil absorption capacity of the superhydrophobic/superoleophilic TiO_2−PVA sponge is further studied. In order to achieve oil/water separation, an oil/water

https://doi.org/10.1021/acsomega.1c06775
ACS Omega 2022, 7, 7084−7095

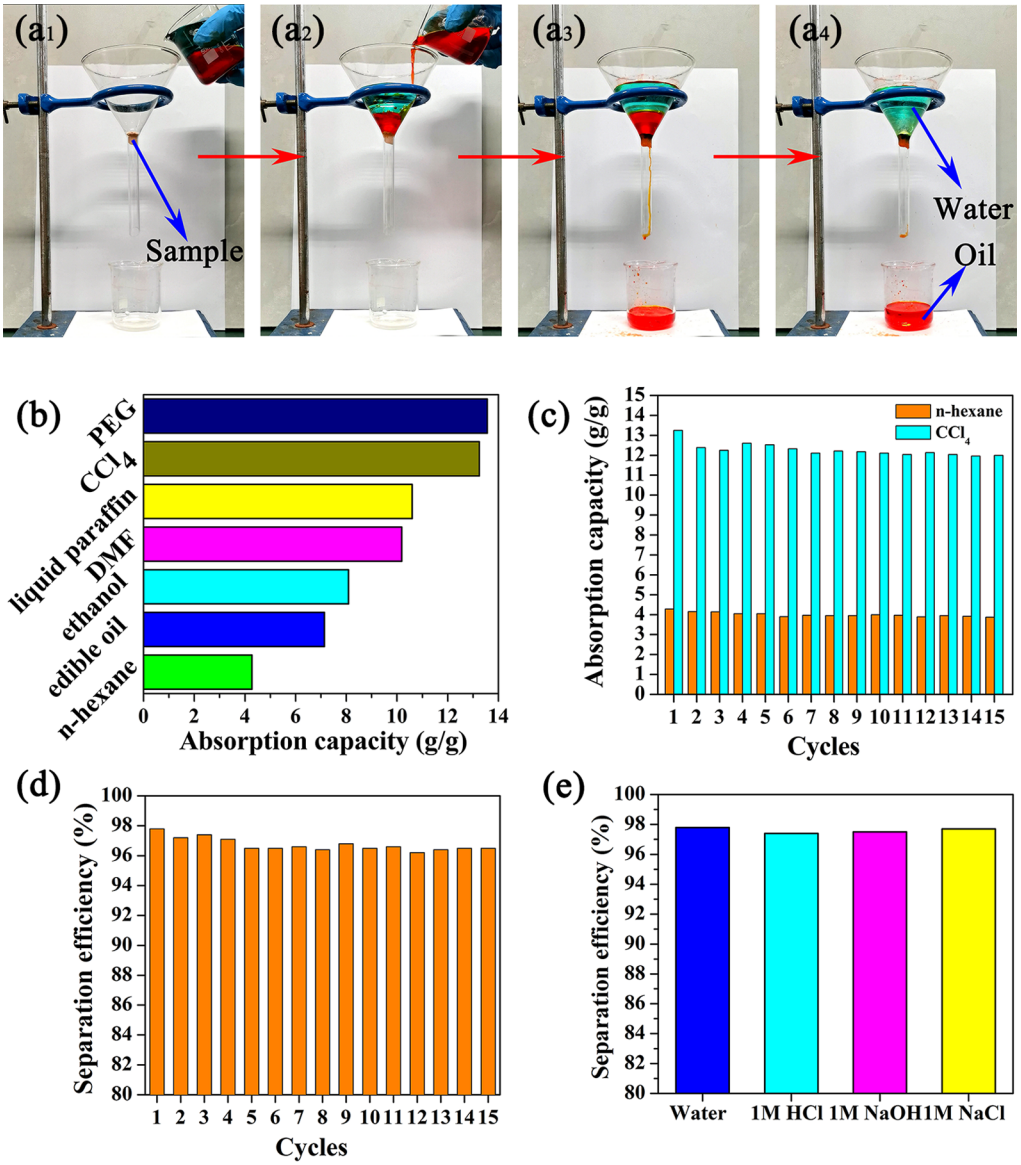

Figure 7. (a1−a4) Separation process of the water (dyed with Brilliant Green) mixture with CCl_4 (dyed with Sudan I) with the TiO_2−PVA sponge; (b) absorption capacity of the TiO_2−PVA sponge for different oils and organic solvents; (c) absorption recyclability of the TiO_2−PVA sponge for *n*-hexane and CCl_4; (d) variation in separation efficiency of the TiO_2−PVA sponge versus the number of oil/water separation cycles. (e) Separation efficiency of the TiO_2−PVA sponge for separating CCl_4 from different corrosive solution mixtures.

Table 1. Comparison of the Adsorption Capacity and Recyclability of PVA-Based Sponges

sponge	modifying materials	adsorbed materials	adsorption capacity (g/g)	recyclability (times)	ref
PVA sponge	poly(acrylic acid), Prussian Blue	c	4.082×10^{-3}		33
PVA sponge	Zn/Fe layered double hydroxide	As (V) anions	8.57×10^{-2}	5	34
PVF sponge	PVA−COOH	water	9.5	10	37
PVF sponge	PVA and chitosan (or diatomite, sodium alginate)	water	6.4−14.6	10	38
PVF sponge	dodecyltrimethoxysilane	oils, organic solvents	4.0−14.0	10	39
PVA sponge	trimethoxy(octadecyl)silane, Na_2SiO_3	oils, organic solvents	1.8−7.0	10	40
PVA sponge	TiO_2, KH550, H_3BO_3, FDTS	oils, organic solvents	4.3−13.6	15	this work

separation device is designed, as exhibited in Figure 7a$_1$−a$_4$. When the mixture of oil (CCl_4 dyed with Sudan I) and water (dyed with Brilliant Green) is poured into the separation device, water is tightly blocked by the TiO_2−PVA sponge sample and oil can easily flow through the TiO_2−PVA sponge into the beaker below. These results indicate the excellent superhydrophobicity and superoleophilicity of the TiO_2−PVA sponge.[24] As shown in Figure 7b, the maximum adsorption capacity of the TiO_2−PVA sponge is evaluated by the adsorption capacity of oils and solvents [i.e., polyethylene glycol (PEG), CCl_4, liquid paraffin, *N*,*N*-dimethylformamide, ethanol, edible oil, and *n*-hexane]. The TiO_2−PVA sponge displays excellent oil adsorption capacities ranging from 4.3 to 13.6 times its own weight, as shown in Table 1, depending on

https://doi.org/10.1021/acsomega.1c06775
ACS Omega 2022, 7, 7084−7095

the density and viscosity of the oil and organic solvents and the porosity of the TiO_2−PVA sponge.[2,23,24,44] Because of abundant hydroxyl groups, the pristine PVA sponge can be modified to possess superhydrophilicity (or superoleophilicity) such that different kinds of wastes (i.e., ions, oils, and/or organic solvents) can be absorbed (Table 1). Compared with PVA-based sponges, other superhydrophobic sponge materials (i.e., PU sponge, melamine sponge, cellulose sponge, and graphene sponge) usually show higher oil adsorption capacities because of different porosities and surface chemistry properties.[68]

In addition, the recyclability of the superhydrophobic/superoleophilic sponge materials for oil/water separation is also an important parameter for the long-term practical oil/water separation. Thus, *n*-hexane and CCl_4 are utilized to investigate the recyclability of the TiO_2−PVA sponge. As presented in Figure 7c, the absorption capacity of the TiO_2−PVA sponge for *n*-hexane and CCl_4 does not show an obvious decrease even after 15 cyclic absorption tests, suggesting that the TiO_2−PVA sponge is an ideal material to separate oils from the water mixture. Furthermore, the calculated separation efficiency of the TiO_2−PVA sponge separating CCl_4 from the water mixture reaches about 97.8%, and the separation efficiency still maintains 96.5% even after 15 cyclic oil/water separations, as shown in the Figure 7d. Besides, the stability of the TiO_2−PVA sponge in corrosive solutions (i.e., 1 M NaOH, 1 M HCl, and 1 M NaCl) is investigated by repeated separation cycles for the mixture of CCl_4 and water. The TiO_2−PVA sponge exhibits a high separation efficiency (∼97.5%) for corrosive oil/water mixtures (Figure 7e). In short, the superhydrophobic/superoleophilic TiO_2−PVA sponge possesses excellent oil/water separation, recyclability, and chemical resistance properties and has great potential in the practical application of treating oily wastewater and oil spills.

2.7. Continuous Separation Capability of the TiO_2−PVA Sponge. In real practical applications, the efficiency of oil adsorption and oil/water separation is of great importance to treat frequent oil spills and large quantities of oily wastewater. Thus, a continuous separation device for oil/water separation is designed with the assistance of a vacuum pump, as shown in Figure 8. The superhydrophobic/superoleophilic TiO_2−PVA sponge is attached to a tube connected with the vacuum pump, and the TiO_2−PVA sponge is placed at the oil/water interface (Figure 8a). After turning on the vacuum pump, the Sudan I-dyed *n*-hexane is continuously pumped into the Büchne flask, as shown in Figure 8b−d, and *n*-hexane in the mixed solution can be completely separated into the Büchne flask in a short time. During a separation process, the TiO_2−PVA sponge retains superhydrophobicity, and there is no water in the collected *n*-hexane. As for the continuous oil/water separation, the saturated absorption problem of superhydrophobic/superoleophilic sponge materials can be automatically solved with the aid of the vacuum pump. For example, Chen et al. found that silylated PVA sponge can achieve a total of 7600 times its own weight by the continuous separation.[36] Wang et al. suggested that oils with high viscosity can be treated by continuous separation.[16] Thus, the continuous oil/water separation shows great potential in dealing with large-scale oil spill accidents.

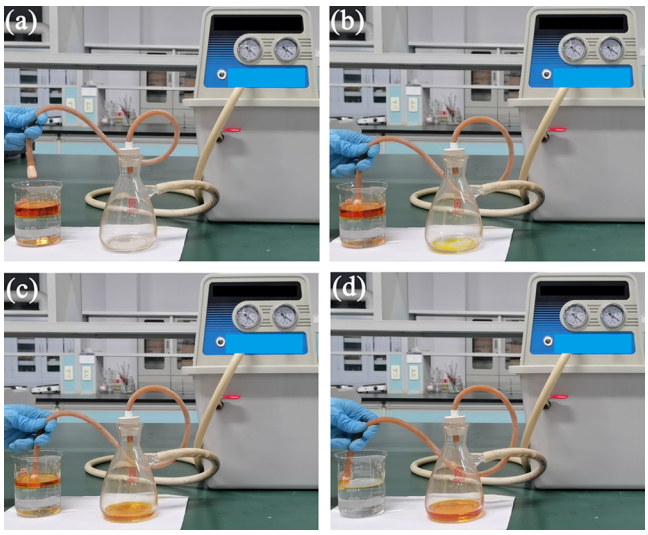

Figure 8. Pictures of vacuum pump-assisted continuous removal of *n*-hexane (dyed with Sudan I) from the water surface.

3. CONCLUSIONS

In summary, a new superhydrophobic/superoleophilic TiO_2−PVA sponge is prepared by firmly anchoring TiO_2 nanoparticles onto the skeletons of the pristine PVA sponge via a cross-linking reaction between TiO_2 and KH550 and H_3BO_3. The as-prepared TiO_2−PVA sponge shows excellent chemical stability, thermal stability, and abrasion resistance in harsh environments. Due to the porosity and superhydrophobicity/superoleophilicity, the absorption capacities of the TiO_2−PVA sponge for various oils and organic solvents range from 4.3 to 13.6 times their own weight. When used in an oil/water separation test, the separation efficiency of the TiO_2−PVA sponge reaches ∼97.8%. Besides, the TiO_2−PVA sponge also exhibits good recyclability with a separation efficiency of ∼96.5% even after 15 cyclic oil/water separation processes. Furthermore, the continuous oil/water separation of the TiO_2−PVA sponge further demonstrates its great potential in practical applications of dealing with oily wastewater and large-scale oil spills. Therefore, the rational design of the superhydrophobic/superoleophilic TiO_2−PVA sponge opens an avenue for preparing new porous sponge materials and also provides new insights into efficient oil/water separation.

4. EXPERIMENTAL SECTION

4.1. Materials. The PVA sponge was purchased from a local supermarket. 3-Aminopropyltriethoxysilane (KH550, 99%), CCl_4 (98%), and boric acid (H_3BO_3, 99.5%) were received from Shanghai Macklin Biochemical Co., Ltd. FDTS and Brilliant Green (CAS: 633-03-4) were purchased from Shanghai Aladdin BioChem Technology Co., Ltd. *n*-Hexane (99.5%) was purchased from Shandong Xiya Chemical Industry Co., Ltd. Sudan I (CAS: 842-07-9) was bought from Sinopharm Chemical Reagent Co., Ltd. TiO_2 nanoparticles (CAS: 13463-67-7) were provided by Hangzhou Hengna New Materials Co., Ltd. Sodium hydroxide (NaOH, 96%) was purchased from Hangzhou Gaojing Fine Chemicals Co., Ltd.

4.2. Preparation of the TiO_2−PVA Sponge. The pristine PVA sponge was first ultrasonically cleaned in an ethanol solution for 30 min and then dried in an oven at 70 °C. Then, 0.12 g TiO_2 nanoparticles were added into 100 mL NaOH

https://doi.org/10.1021/acsomega.1c06775
ACS Omega 2022, 7, 7084−7095

aqueous solution (pH = 10), followed by mixing and magnetically stirring for 2 h to obtain a suspension solution of TiO_2 nanoparticles. Subsequently, 1 g H_3BO_3 was added into the above suspension solution, and the mixed solution was stirred for another 2 h at 85 °C. After that, 0.5 g KH550 was added to the above mixed solution, and the pre-cleaned PVA sponge was immersed in the solution. The reaction was kept at 85 °C for 3 h under stirring, and the resulting PVA sponge was taken out and dried in an oven at 60 °C. Finally, the resulting PVA sponge was immersed in a solution of FDTS in *n*-hexane (0.5 wt %) for 30 min and dried at 80 °C for 2 h to obtain a superhydrophobic TiO_2−PVA sponge.

4.3. Characterization. A scanning electron microscope (Apreo, FEI) was used to analyze the morphologies of the pristine PVA sponge and the as-prepared superhydrophobic/superoleophilic TiO_2−PVA sponge. The chemical composition of the TiO_2−PVA sponge was measured by EDS and FTIR (Nicolet iS 10, Thermo Fisher). The surface crystal structures of the superhydrophobic TiO_2−PVA sponge were characterized by X-ray diffraction (XRD, SMART LAB, Rigaku). The WCA was tested and repeated with a deionized water droplet of ∼5 μL by using a contact angle goniometer (DSA25, KRüSS) at room temperature.[69−72] The size distribution of TiO_2 nanoparticle dispersion was characterized by using dynamic light scattering (Nano BT-90).

4.4. Stability Measurements. The chemical stability of the TiO_2−PVA sponge was tested by immersing the TiO_2−PVA sponge in different solutions (i.e., *n*-hexane, CCl_4, and ethanol) for 24 h and different pH solutions (i.e., pH = 1, pH = 7, and pH = 13) for 25 h. To assess the thermal stability, the TiO_2−PVA sponge was immersed in boiling water for different times (0−60 min). Furthermore, to evaluate the sustainability of the superhydrophobic/superoleophilic TiO_2−PVA sponge, WCAs were tested after sandpaper abrasion tests. The TiO_2−PVA sponge was pressed against an 800 mesh sandpaper with a 100 g stainless weight and was then pulled by a pair of tweezers at a speed of 0.1 cm/s. Besides, the durability of the TiO_2−PVA sponge was also tested by ultrasonification (Kunshan Ultrasonic Instrument, 150 W). The TiO_2−PVA sponge is first ultrasonified for a certain time (i.e., 0−60 min) and then dried in an oven, followed by evaluating the contact angles of a droplet on the TiO_2−PVA sponge.

4.5. Oil Absorption Experiments. In order to evaluate the absorption capacity of the TiO_2−PVA sponge, a piece of the superhydrophobic/superoleophilic TiO_2−PVA sponge was immersed in various solvents and oils (i.e., PEG, CCl_4, liquid paraffin, ethanol, edible oil, and *n*-hexane) for 1 min until the sponges were saturated with liquids, and then the weight of the saturated sponges was measured. The absorption capacity (Q) was calculated by the following equation

$$Q = (M_1 - M_0)/M_0 \quad (1)$$

where M_0 (g) and M_1 (g) represent the weight of the TiO_2−PVA sponge before and after absorption, respectively. The recyclability of the TiO_2−PVA sponge was characterized by the following process. After finishing an absorption process, the TiO_2−PVA sponge was washed by anhydrous ethanol and then dried in an oven at 60 °C. The above process was repeated 15 times to evaluate the recyclability of the TiO_2−PVA sponge.

4.6. Oil/Water Separation Experiment. A self-made device was used for the oil/water separation experiment. The superhydrophobic/superoleophilic TiO_2−PVA sponge was first fixed in a funnel. Then, the mixture of water and CCl_4 was poured into the funnel to realize the separation of oil from water. In this process, water was repelled by the TiO_2−PVA sponge in the funnel, while oil could easily leak through the TiO_2−PVA sponge because of its superhydrophobicity and superoleophilicity. The separation efficiency (η) was calculated by the following equation

$$\eta = (M_b/M_a) \times 100\% \quad (2)$$

where M_a (g) and M_b (g) are the weight of the oil before and after oil/water separation, respectively, and η (%) is the separation efficiency of the TiO_2−PVA sponge.

4.7. Continuous In Situ Oil/Water Separation. A continuous oil/water separation device was designed by using a vacuum pump system consisting of a Büchne flask and rubber tube. One end of the rubber tube was attached to the superhydrophobic/superoleophilic TiO_2−PVA sponge, and the other end was connected to the Büchne flask. In this test, the sponge was immersed in the oil/water interface of the mixture solution, and the oil/water separation was continuously carried out with the aid of a vacuum pump.

■ ASSOCIATED CONTENT

Supporting Information

The Supporting Information is available free of charge at https://pubs.acs.org/doi/10.1021/acsomega.1c06775.

Photo images of WCAs on the TiO_2−PVA sponge after ultrasonification in ethanol for different times and the size distribution of TiO_2 nanoparticle dispersion by using the DLS measurement (PDF)

■ AUTHOR INFORMATION

Corresponding Author

Zhiwei He − *Center for Advanced Optoelectronic Materials, Anti-Icing Materials (AIM) Laboratory, College of Materials and Environmental Engineering, Hangzhou Dianzi University, Hangzhou 310018, China;* orcid.org/0000-0002-3251-8731; Email: zhiwei.he@hdu.edu.cn

Authors

Hanqing Wu − *School of Mechanical Engineering, Hangzhou Dianzi University, Hangzhou 310018, China*

Zhen Shi − *Institute of Advanced Magnetic Materials, College of Materials and Environmental Engineering, Hangzhou Dianzi University, Hangzhou 310012, China;* orcid.org/0000-0002-5354-1703

Zhe Kong − *Center for Advanced Optoelectronic Materials, Anti-Icing Materials (AIM) Laboratory, College of Materials and Environmental Engineering, Hangzhou Dianzi University, Hangzhou 310018, China;* orcid.org/0000-0001-8622-0175

Shiyu Ma − *Center for Advanced Optoelectronic Materials, Anti-Icing Materials (AIM) Laboratory, College of Materials and Environmental Engineering, Hangzhou Dianzi University, Hangzhou 310018, China*

Yuping Sun − *Center for Advanced Optoelectronic Materials, Anti-Icing Materials (AIM) Laboratory, College of Materials and Environmental Engineering, Hangzhou Dianzi University, Hangzhou 310018, China*

Xianguo Liu − *Institute of Advanced Magnetic Materials, College of Materials and Environmental Engineering, Hangzhou Dianzi University, Hangzhou 310012, China*

https://doi.org/10.1021/acsomega.1c06775
ACS Omega 2022, 7, 7084−7095

Complete contact information is available at:
https://pubs.acs.org/10.1021/acsomega.1c06775

Notes

The authors declare no competing financial interest.

■ ACKNOWLEDGMENTS

The authors acknowledge the National Natural Science Foundation of China (grant no. 51803043), the Science Foundation of Hangzhou Dianzi University (KYS205620119), and the Fundamental Research Funds for the Provincial Universities of Zhejiang (GK209907299001-009) for financial support.

■ REFERENCES

(1) Yu, T.; Halouane, F.; Mathias, D.; Barras, A.; Wang, Z.; Lv, A.; Lu, S.; Xu, W.; Meziane, D.; Tiercelin, N.; Szunerits, S.; Boukherroub, R. Preparation of magnetic, superhydrophobic/superoleophilic polyurethane sponge: Separation of oil/water mixture and demulsification. *Chem. Eng. J.* **2020**, *384*, 123339.
(2) Parsaie, A.; Mohammadi-Khanaposhtani, M.; Riazi, M.; Tamsilian, Y. Magnesium stearate-coated superhydrophobic sponge for oil/water separation: Synthesis, properties, application. *Sep. Purif. Technol.* **2020**, *251*, 117105.
(3) Chen, X.; Weibel, J. A.; Garimella, S. V. Continuous oil−water separation using polydimethylsiloxane-functionalized melamine sponge. *Ind. Eng. Chem. Res.* **2016**, *55*, 3596−3602.
(4) Saleem, J.; Adil Riaz, M.; Gordon, M. Oil sorbents from plastic wastes and polymers: A review. *J. Hazard. Mater.* **2018**, *341*, 424−437.
(5) Peng, J.; Deng, J.; Quan, Y.; Yu, C.; Wang, H.; Gong, Y.; Liu, Y.; Deng, W. Superhydrophobic melamine sponge coated with striped polydimethylsiloxane by thiol−ene click reaction for efficient oil/water separation. *ACS Omega* **2018**, *3*, 5222−5228.
(6) Wang, Z.; Ji, S.; He, F.; Cao, M.; Peng, S.; Li, Y. One-step transformation of highly hydrophobic membranes into superhydrophilic and underwater superoleophobic ones for high-efficiency separation of oil-in-water emulsions. *J. Mater. Chem. A* **2018**, *6*, 3391−3396.
(7) Wang, H.; He, M.; Liu, H.; Guan, Y. One-step fabrication of robust superhydrophobic steel surfaces with mechanical durability, thermal stability, and anti-icing function. *ACS Appl. Mater. Interfaces* **2019**, *11*, 25586−25594.
(8) He, Z.; Zhuo, Y.; Zhang, Z.; He, J. Design of icephobic surfaces by lowering ice adhesion strength: A mini review. *Coatings* **2021**, *11*, 1343.
(9) He, Z.; Xiao, S.; Gao, H.; He, J.; Zhang, Z. Multiscale crack initiator promoted super-low ice adhesion surfaces. *Soft Matter* **2017**, *13*, 6562−6568.
(10) He, Z.; Jamil, M. I.; Li, T.; Zhang, Q. Enhanced surface icephobicity on an elastic substrate. *Langmuir* **2022**, *38*, 18−35.
(11) Caldona, E. B.; De Leon, A. C. C.; Thomas, P. G.; Naylor, D. F.; Pajarito, B. B.; Advincula, R. C. Superhydrophobic rubber-modified polybenzoxazine/SiO_2 nanocomposite coating with anticorrosion, anti-ice, and superoleophilicity properties. *Ind. Eng. Chem. Res.* **2017**, *56*, 1485−1497.
(12) Kazemi, K. K.; Zarifi, T.; Mohseni, M.; Narang, R.; Golovin, K.; Zarifi, M. H. Smart superhydrophobic textiles utilizing a long-range antenna sensor for hazardous aqueous droplet detection plus prevention. *ACS Appl. Mater. Interfaces* **2021**, *13*, 34877−34888.
(13) He, Z.; He, J.; Zhang, Z. Selective growth of metallic nanostructures on microstructured copper substrate in solution. *CrystEngComm* **2015**, *17*, 7262−7269.
(14) He, Z.; Zhang, Z.; He, J. CuO/Cu based superhydrophobic and self-cleaning surfaces. *Scr. Mater.* **2016**, *118*, 60−64.
(15) Marlena, J.; Tan, J. K. S.; Lin, Z.; Li, D. X.; Zhao, B.; Leo, H. L.; Kim, S.; Yap, C. H. Monolithic polymeric porous superhydrophobic material with pneumatic plastron stabilization for functionally durable drag reduction in blood-contacting biomedical applications. *NPG Asia Mater.* **2021**, *13*, 58.
(16) Wang, Y.; Zhu, Y.; Yang, C.; Liu, J.; Jiang, W.; Liang, B. Facile two-step strategy for the construction of a mechanically stable three-dimensional superhydrophobic structure for continuous oil−water separation. *ACS Appl. Mater. Interfaces* **2018**, *10*, 24149−24156.
(17) You, Q.; Ran, G.; Wang, C.; Zhao, Y.; Song, Q. Facile fabrication of superhydrophilic and underwater superoleophobic chitosan−polyvinyl alcohol-TiO_2 coated copper mesh for efficient oil/water separation. *J. Coat. Technol. Res.* **2018**, *15*, 1013−1023.
(18) Cai, Y.; Wu, Y.; Yang, F.; Gan, J.; Wang, Y.; Zhang, J. Wood sponge reinforced with polyvinyl alcohol for sustainable oil−water separation. *ACS Omega* **2021**, *6*, 12866−12876.
(19) Chen, K.; Gou, W.; Wang, X.; Zeng, C.; Ge, F.; Dong, Z.; Wang, C. UV-cured fluoride-free polyurethane functionalized textile with pH-induced switchable superhydrophobicity and underwater superoleophobicity for controllable oil/water separation. *ACS Sustainable Chem. Eng.* **2018**, *6*, 16616−16628.
(20) Khanjani, P.; King, A. W. T.; Partl, G. J.; Johansson, L.-S.; Kostiainen, M. A.; Ras, R. H. A. Superhydrophobic paper from nanostructured fluorinated cellulose esters. *ACS Appl. Mater. Interfaces* **2018**, *10*, 11280−11288.
(21) Zhang, W.; Liu, N.; Cao, Y.; Lin, X.; Liu, Y.; Feng, L. Superwetting porous materials for wastewater treatment: from immiscible oil/water mixture to emulsion separation. *Adv. Mater. Interfaces* **2017**, *4*, 1600029.
(22) Zhang, Q.; Liu, H.; Zhan, X.; Chen, F.; Yan, J.; Tang, H. Microstructure and antibacterial performance of functionalized polyurethane based on polysiloxane tethered cationic biocides. *RSC Adv.* **2015**, *5*, 77508−77517.
(23) Li, Z.-T.; Wu, H.-T.; Chen, W.-Y.; He, F.-A.; Li, D.-H. Preparation of magnetic superhydrophobic melamine sponges for effective oil-water separation. *Sep. Purif. Technol.* **2019**, *212*, 40−50.
(24) Li, Y.; Zhang, G.; Gao, A.; Cui, J.; Zhao, S.; Yan, Y. Robust graphene/poly(vinyl alcohol) janus aerogels with a hierarchical architecture for highly efficient switchable separation of oil/water emulsions. *ACS Appl. Mater. Interfaces* **2019**, *11*, 36638−36648.
(25) Zhu, J.; Jiang, J.; Jamil, M. I.; Hou, Y.; Zhan, X.; Chen, F.; Cheng, D.; Zhang, Q. Biomass-derived, water-induced self-recoverable composite aerogels with robust superwettability for water treatment. *Langmuir* **2020**, *36*, 10960−10969.
(26) Zhang, G.; Li, Y.; Gao, A.; Zhang, Q.; Cui, J.; Zhao, S.; Zhan, X.; Yan, Y. Bio-inspired underwater superoleophobic PVDF membranes for highly-efficient simultaneous removal of insoluble emulsified oils and soluble anionic dyes. *Chem. Eng. J.* **2019**, *369*, 576−587.
(27) Zhang, Q.; Jiang, J.; Gao, F.; Zhang, G.; Zhan, X.; Chen, F. Engineering high-effective antifouling polyether sulfone membrane with P(PEG-PDMS-KH570)@SiO_2 nanocomposite via in-situ sol-gel process. *Chem. Eng. J.* **2017**, *321*, 412−423.
(28) Zhang, G.; Jiang, J.; Zhang, Q.; Zhan, X.; Chen, F. Amphiphilic poly(ether sulfone) membranes for oil/water separation: Effect of sequence structure of the modifier. *AIChE J.* **2017**, *63*, 739−750.
(29) Fu, Y.; Jin, B.; Zhang, Q.; Zhan, X.; Chen, F. pH-induced switchable superwettability of efficient antibacterial fabrics for durable selective oil/water separation. *ACS Appl. Mater. Interfaces* **2017**, *9*, 30161−30170.
(30) Liu, H.; Kang, Y. Superhydrophobic and superoleophilic modified EPDM foam rubber fabricated by a facile approach for oil/water separation. *Appl. Surf. Sci.* **2018**, *451*, 223−231.
(31) Chang, Y.-I.; Chen, J.-W.; Cheng, W.-Y.; Jang, L. The reinforcement of the physical strength of PVA sponge through the double acetalization. *Sep. Purif. Technol.* **2018**, *198*, 100−107.
(32) Kim, H.; Lee, Y.; Kim, Y.; Hwang, Y.; Hwang, N. Biomimetically reinforced polyvinyl alcohol-based hybrid scaffolds for cartilage tissue engineering. *Polymers* **2017**, *9*, 655.
(33) Wi, H.; Kim, H.; Oh, D.; Bae, S.; Hwang, Y. Surface modification of poly(vinyl alcohol) sponge by acrylic acid to

https://doi.org/10.1021/acsomega.1c06775
ACS Omega 2022, 7, 7084−7095

immobilize Prussian blue for selective adsorption of aqueous cesium. *Chemosphere* **2019**, *226*, 173−182.
(34) Dai, X.; Zhang, S.; Waterhouse, G. I. N.; Fan, H.; Ai, S. Recyclable polyvinyl alcohol sponge containing flower-like layered double hydroxide microspheres for efficient removal of As(V) anions and anionic dyes from water. *J. Hazard. Mater.* **2019**, *367*, 286−292.
(35) Guo, M.; Zhang, Y.; Du, F.; Wu, Y.; Zhang, Q.; Jiang, C. Silver nanoparticles/polydopamine coated polyvinyl alcohol sponge as an effective and recyclable catalyst for reduction of 4-nitrophenol. *Mater. Chem. Phys.* **2019**, *225*, 42−49.
(36) Chen, J.; Xiang, J.; Yue, X.; Li, H.; Yu, X. Synthesis of a superhydrophobic polyvinyl alcohol sponge using water as the only solvent for continuous oil-water separation. *J. Chem.* **2019**, *2019*, 7153109.
(37) Sha, D.; Zheng, R.; Wang, B.; Shi, K.; Yang, X.; Liu, X.; Liu, Z.; Ji, X. Three-dimensional superhydrophilic polyvinyl alcohol−formaldehyde composite sponges with suitable pore sizes for high efficiency emulsion separation. *New J. Chem.* **2021**, *45*, 17816−17826.
(38) Sha, D.; Zheng, R.; Wang, B.; Xu, J.; Shi, K.; Yang, X.; Ji, X. Superhydrophilic polyvinyl alcohol-formaldehyde composite sponges with hierachical pore structure for oil/water emulsion separation. *React. Funct. Polym.* **2021**, *165*, 104975.
(39) Wang, B.; Yang, X.; Sha, D.; Shi, K.; Xu, J.; Ji, X. Silane functionalized polyvinyl-alcohol formaldehyde sponges on fast oil absorption. *ACS Appl. Polym. Mater.* **2020**, *2*, 5309−5317.
(40) Wang, Q.; Li, Q.; Yasir Akram, M.; Ali, S.; Nie, J.; Zhu, X. Decomposable polyvinyl alcohol-based super-hydrophobic three-dimensional porous material for effective water/oil separation. *Langmuir* **2018**, *34*, 15700−15707.
(41) Wang, Y.; Shang, B.; Hu, X.; Peng, B.; Deng, Z. Temperature control of mussel-inspired chemistry toward hierarchical superhydrophobic surfaces for oil/water separation. *Adv. Mater. Interfaces* **2017**, *4*, 1600727.
(42) Shang, B.; Wang, Y.; Peng, B.; Deng, Z. Bioinspired polydopamine particles-assisted construction of superhydrophobic surfaces for oil/water separation. *J. Colloid Interface Sci.* **2016**, *482*, 240−251.
(43) Wang, N.; Wang, Y.; Shang, B.; Wen, P.; Peng, B.; Deng, Z. Bioinspired one-step construction of hierarchical superhydrophobic surfaces for oil/water separation. *J. Colloid Interface Sci.* **2018**, *531*, 300−310.
(44) Pan, Y.; Shi, K.; Peng, C.; Wang, W.; Liu, Z.; Ji, X. Evaluation of hydrophobic polyvinyl-alcohol formaldehyde sponges as absorbents for oil spill. *ACS Appl. Mater. Interfaces* **2014**, *6*, 8651−8659.
(45) Jannatun, N.; Taraqqi-A-Kamal, A.; Rehman, R.; Kuker, J.; Lahiri, S. K. A facile cross-linking approach to fabricate durable and self-healing superhydrophobic coatings of SiO2-PVA@PDMS on cotton textile. *Eur. Polym. J.* **2020**, *134*, 109836.
(46) Lahiri, S. K.; Zhang, P.; Zhang, C.; Liu, L. Robust fluorine-free and self-healing superhydrophobic coatings by H_3BO_3 incorporation with SiO_2−alkyl-silane@PDMS on cotton fabric. *ACS Appl. Mater. Interfaces* **2019**, *11*, 10262−10275.
(47) Zhang, Z.; Pan, H.; Liu, P.; Zhao, M.; Li, X.; Zhang, Z. Boric acid incorporated on the surface of reactive nanosilica providing a nano-crosslinker with potential in guar gum fracturing fluid. *J. Appl. Polym. Sci.* **2017**, *134*, 45037.
(48) Zhang, Z.; Liu, P.; Pan, H.; Zhao, M.; Li, X.; Zhang, Z. Preparation of a nanosilica cross-linker and investigation of its effect on properties of guar gum fracturing fluid. *Micro Nano Lett.* **2017**, *12*, 445−449.
(49) Hdidar, M.; Chouikhi, S.; Fattoum, A.; Arous, M.; Kallel, A. Influence of TiO_2 rutile doping on the thermal and dielectric properties of nanocomposite films based PVA. *J. Alloys Compd.* **2018**, *750*, 375−383.
(50) Chen, X. Preparation and property of TiO_2 nanoparticle dispersed polyvinyl alcohol composite materials. *J. Mater. Sci. Lett.* **2002**, *21*, 1637−1639.
(51) Lee, J.; Hong, J.; Park, D. W.; Shim, S. E. Microencapsulation and characterization of poly(vinyl alcohol)-coated titanium dioxide particles for electrophoretic display. *Opt. Mater.* **2010**, *32*, 530−534.
(52) Zhang, Y.; Zhu, P. C.; Edgren, D. Crosslinking reaction of poly(vinyl alcohol) with glyoxal. *J. Polym. Res.* **2010**, *17*, 725−730.
(53) Sonker, A. K.; Rathore, K.; Nagarale, R. K.; Verma, V. Crosslinking of polyvinyl alcohol (PVA) and effect of crosslinker shape (aliphatic and aromatic) thereof. *J. Polym. Environ.* **2018**, *26*, 1782−1794.
(54) Aziz, S. B.; Hassan, A. Q.; Mohammed, S. J.; Karim, W. O.; Kadir, M. F. Z.; Chan, N. N. M. Y.; Chan, N. M. Y. Structural and optical characteristics of PVA:C-dot composites: Tuning the absorption of ultra violet (UV) region. *Nanomaterials* **2019**, *9*, 216.
(55) Chandrakala, H. N.; Ramaraj, B.; Shivakumaraiah; Madhu, G. M.; Siddaramaiah. The influence of zinc oxide−cerium oxide nanoparticles on the structural characteristics and electrical properties of polyvinyl alcohol films. *J. Mater. Sci.* **2012**, *47*, 8076−8084.
(56) Das, M.; Sarkar, D. Development of room temperature ethanol sensor from polypyrrole (PPy) embedded in polyvinyl alcohol (PVA) matrix. *Polym. Bull.* **2018**, *75*, 3109−3125.
(57) Weng, D.; Xu, F.; Li, X.; Li, Y.; Sun, J. Bioinspired photothermal conversion coatings with self-healing superhydrophobicity for efficient solar steam generation. *J. Mater. Chem. A* **2018**, *6*, 24441−24451.
(58) Yadav, V.; Verma, P.; Sharma, H.; Tripathy, S.; Saini, V. K. Photodegradation of 4-nitrophenol over B-doped TiO_2 nanostructure: effect of dopant concentration, kinetics, and mechanism. *Environ. Sci. Pollut. Res.* **2020**, *27*, 10966−10980.
(59) Feng, N.; Zheng, A.; Wang, Q.; Ren, P.; Gao, X.; Liu, S.-B.; Shen, Z.; Chen, T.; Deng, F. Boron environments in B-doped and (B, N)-codoped TiO_2 photocatalysts: A combined solid-state NMR and theoretical calculation study. *J. Phys. Chem. C* **2011**, *115*, 2709−2719.
(60) Yang, Z.; Feng, X.; Xu, M.; Rodrigue, D. Properties of poplar fiber/PLA composites: Comparison on the effect of maleic anhydride and KH550 modification of poplar fiber. *Polymers* **2020**, *12*, 729.
(61) Teng, Y.; Wang, Y.; Shi, B.; Fan, W.; Li, Z.; Chen, Y. Facile fabrication of superhydrophobic paper with durability, chemical stability and self-cleaning by roll coating with modified nano-TiO_2. *Appl. Nanosci.* **2020**, *10*, 4063−4073.
(62) Baidya, A.; Ganayee, M. A.; Jakka Ravindran, S.; Tam, K. C.; Das, S. K.; Ras, R. H. A.; Pradeep, T. Organic solvent-free fabrication of durable and multifunctional superhydrophobic paper from waterborne fluorinated cellulose nanofiber building blocks. *ACS Nano* **2017**, *11*, 11091−11099.
(63) Rajendran, S.; Sivakumar, M.; Subadevi, R. Effect of salt concentration in poly(vinyl alcohol)-based solid polymer electrolytes. *J. Power Sources* **2003**, *124*, 225−230.
(64) Malathi, J.; Kumaravadivel, M.; Brahmanandhan, G. M.; Hema, M.; Baskaran, R.; Selvasekarapandian, S. Structural, thermal and electrical properties of PVA−$LiCF_3SO_3$ polymer electrolyte. *J. Non-Cryst. Solids* **2010**, *356*, 2277−2281.
(65) Freyman, C. A.; Chung, Y.-W. Synthesis and characterization of hardness-enhanced multilayer oxide films for high-temperature applications. *Surf. Coat. Technol.* **2008**, *202*, 4702−4708.
(66) Zhou, Y.; Zhang, N.; Zhou, X.; Hu, Y.; Hao, G.; Li, X.; Jiang, W. Design of recyclable superhydrophobic PU@Fe_3O_4@PS sponge for removing oily contaminants from water. *Ind. Eng. Chem. Res.* **2019**, *58*, 3249−3257.
(67) Wang, H.; Yang, J.; Liu, X.; Tao, Z.; Wang, Z.; Yue, R. A robust 3D superhydrophobic sponge for in situ continuous oil removing. *J. Mater. Sci.* **2019**, *54*, 1255−1266.
(68) Sam, E. K.; Liu, J.; Lv, X. Surface engineering materials of superhydrophobic sponges for oil/water separation: A review. *Ind. Eng. Chem. Res.* **2021**, *60*, 2353−2364.
(69) He, Z.; Zhuo, Y.; Wang, F.; He, J.; Zhang, Z. Design and preparation of icephobic PDMS-based coatings by introducing an aqueous lubricating layer and macro-crack initiators at the ice-substrate interface. *Prog. Org. Coat.* **2020**, *147*, 105737.

https://doi.org/10.1021/acsomega.1c06775
ACS Omega 2022, 7, 7084−7095

(70) He, Z.; Vågenes, E. T.; Delabahan, C.; He, J.; Zhang, Z. Room temperature characteristics of polymer-based low ice adhesion surfaces. *Sci. Rep.* **2017**, *7*, 42181.
(71) He, Z.; Zhuo, Y.; He, J.; Zhang, Z. Design and preparation of sandwich-like PDMS sponges with super-low ice adhesion. *Soft Matter* **2018**, *14*, 4846−4851.
(72) He, Z.; Zhuo, Y.; Wang, F.; He, J.; Zhang, Z. Understanding the role of hollow sub-surface structures in reducing ice adhesion strength. *Soft Matter* **2019**, *15*, 2905−2910.

https://doi.org/10.1021/acsomega.1c06775
ACS Omega 2022, 7, 7084−7095